

Fibroblast growth factor 23 exacerbates cardiac fibrosis in deoxycorticosterone acetate -salt hypertensive mice

Tomohiro Saito¹, Masahide Mizobuchi^{1, #}, Tadashi Kato¹, Hiroaki Ogata², Fumihiko Koiwa³,
Hirokazu Honda¹

¹ Division of Nephrology, Department of Medicine, Showa University School of Medicine, Tokyo, Japan. ² Department of Internal Medicine, Showa University Northern Yokohama Hospital, Yokohama, Japan. ³ Division of Nephrology, Department of Medicine, Showa University Fujigaoka Hospital, Yokohama, Japan.

Running title: Cardiac effect of FGF23

Word count: 3536 words

Abstract word count: 205 words

Table: 1; Figures: 6; Supplementary Figures: 2

Corresponding Author.

Division of Nephrology, Department of Medicine Showa University School of Medicine 1-5-8

Hatanodai, Shinagawa-ku, Tokyo 142-8666, Japan

Tel: +81-3-3784-8533

Fax: +81-3-3784-5934

E-mail: mizobu@med.showa-u.ac.jp

Abstract

Fibroblast growth factor 23 (FGF23) is associated with cardiovascular disease in patients with chronic kidney disease (CKD), but the mechanisms underlying the effect of FGF23 on cardiac function remain to be investigated. Herein, we studied the effect of continuous intravenous (CIV) FGF23 loading in a deoxycorticosterone acetate (DOCA)-salt mouse model that has mild CKD and hypertension, and heart failure with a preserved ejection fraction (HFpEF). Wild-type male mice were allocated randomly to four groups: normal control, vehicle-treated DOCA-salt mice, FGF23-treated DOCA-salt mice, and FGF23 and calcitriol-treated DOCA-salt mice. The DOCA-salt mice received agents by CIV for ten days via an infusion mini-pump. DOCA-salt mice that received FGF23 showed a marked increase in serum FGF23, and echocardiography in these mice revealed HFpEF. These mice also showed exacerbation of myocardial fibrosis concomitant with an inverse and significant correlation with *Cyp27b1* expression. Calcitriol treatment attenuated the FGF23-induced cardiac fibrosis and improved diastolic function via inhibition of transforming growth factor (TGF) β signaling. This effect was independent of systemic and local FGF23 levels. These results suggest that CIV FGF23 loading exacerbates cardiac fibrosis and that locally abnormal vitamin D metabolism might be involved in this mechanism. Calcitriol attenuates this exacerbation by mediating TGF β signaling independent of FGF23 levels.

Keywords

fibroblast growth factor 23, calcitriol, heart failure with preserved ejection fraction, transforming growth factor, cardiac fibrosis

Introduction

Chronic kidney disease (CKD) is a global public health epidemic that increases the risks of cardiovascular disease (CVD) and death^{1,2}. Cardiac fibrosis and left ventricular hypertrophy (LVH) are common features of cardiomyopathies that contribute to cardiovascular mortality in patients with CKD³. The cardiorenal interaction has mainly been studied in heart failure with reduced ejection fraction. However, renal impairment is observed in many patients with heart failure with preserved ejection fraction (HFpEF) and is associated with an increased risk of mortality⁴⁻⁶. Interestingly, CKD was also recently identified as a risk factor for developing HFpEF⁷. Pathological processes in CKD, such as vascular changes^{8,9}, dysregulation of factors produced in the kidney¹⁰⁻¹², and impairment of renal filtration¹³, may contribute to development of HFpEF.

Elevated circulating FGF23, an endocrine hormone primarily secreted by osteocytes that reduces serum 1,25-dihydroxyvitamin D₃ [1,25(OH)₂D₃] (calcitriol), the active form of vitamin D (VD); and Klotho deficiency are two early and common metabolic complications of CKD that are both strongly associated with a greater risk of CVD events and mortality¹⁴⁻¹⁷. The classic actions of FGF23 in mineral metabolism include increasing renal phosphate (P) excretion and reduction of circulating levels of calcitriol through inhibition of cytochrome P450 (Cyp) 27b1 and stimulation of Cyp24a1¹⁸. Cyp27b1 is responsible for converting 25(OH)D₃ to 1,25(OH)₂D₃^{19,20}; thus, *Cyp27b1* gene knockout results in calcitriol deficiency²¹. These studies suggest that elevated FGF23 and calcitriol deficiency have crucial roles in adverse outcomes in CKD. Patients with CKD also have significant associations of elevated FGF23 with impaired flow-mediated dilation, arterial stiffness, atherosclerosis, and LVH^{22,23}. However, the roles of circulating and/or cardiac FGF23 in progression of cardiac fibrosis remain to be studied²⁴.

Calcitriol initiates biological responses by binding to the cytoplasmic VD receptor (VDR), which modulates transcription of a number of genes²⁵. Deficiency of calcitriol is an important consequence of elevated FGF23 in CKD²⁶ and is associated with death and CVD, including LVH²⁷. Clinical studies suggest a cardioprotective benefit of active VD therapy in CKD^{28,29}. In contrast, in the PRIMO trial, 48 weeks of treatment with paricalcitol in a CKD cohort with preserved systolic function neither resulted in improved diastolic function nor reduced left ventricular mass³⁰. However, cardiac MRI showed that a minority of the patients had LVH at baseline, possibly explaining the lack of a beneficial effect.

Experimental studies have shown that VD metabolites reduce the expression of genes involved in the development of cardiac hypertrophy and that administration of calcitriol blocks cardiac hypertrophy in rodents and isolated cardiac myocytes^{31,32}. In *Cyp27b1* gene knockout mice, calcitriol deficiency exacerbates radiation-induced bone marrow injury³³ and also worsens bleomycin-induced pulmonary fibrosis, partly through aggravating the transforming growth factor (TGF) β /Smad2/3-mediated epithelial-mesenchymal transition³⁴. These results suggest that calcitriol deficiency and lack of *Cyp27b1* may be associated with progression of local organ fibrosis; however, the role of local VD metabolism in cardiac fibrosis remains to be studied. In this study, we investigated the relationship between FGF23 loading and cardiac VD metabolism in a deoxycorticosterone acetate (DOCA)-salt mouse model, which has been used as a model of HFpEF³⁵⁻³⁸.

Methods

Experimental protocol

All studies were approved by the Showa University Animal Studies Committee in accordance with federal regulations. The DOCA-salt mouse model of hypertension was used because it involves primarily diastolic, rather than systolic, impairment and recapitulates the following aspects of human HFpEF³⁵⁻³⁸: pulmonary congestion, preserved left ventricular (LV) ejection fraction (LVEF), diastolic dysfunction (DD), LVH, moderate hypertension, and exercise intolerance³⁹⁻⁴¹. Male wild-type mice (22-25 g; 8 weeks old; Charles River Laboratories, Japan) in a C57BL/6 background were housed in a temperature-controlled environment. The mice (n = 16) were allocated randomly to four groups: wild type mice used as normal controls (group NC, n = 4); vehicle-treated DOCA-salt mice (group V, n = 4); FGF23-treated DOCA-salt mice (group F, n = 4); FGF23 and calcitriol-treated DOCA-salt mice (group C, n = 4). DOCA-salt mice were anesthetized with sodium pentobarbital intraperitoneally (i.p.) (50 mg/kg). These mice received DOCA from subcutaneous pellets (50 mg/pellet; Innovative Research of America, Sarasota, FL, USA) and nephrectomy (Nx) was performed simultaneously on the left kidney. All mice were maintained on 0.9% sodium chloride drinking water and fed a regular diet^{42,43}. Experiments were started one week after Nx to allow time for recovery. At this time, a micro-infusion pump (iPRECIO® model SMP-300, Primetech Corp., Tokyo, Japan), which permits quantitative pharmacology in the right jugular vein using a catheter in single animals, was implanted into the DOCA-salt mice to allow continuous intravenous (CIV) infusion of reagents. Mice were infused with phosphate-buffered saline (PBS) for 4 days after implantation, followed by CIV infusion of PBS (group V), recombinant mouse FGF23 (80 µg/kg/day; R&D Systems, Inc., Minneapolis, MN, USA; group F), or recombinant FGF23 and

calcitriol (0.4 $\mu\text{g}/\text{kg}/\text{day}$ i.p. three times per week) (group C) for 10 days. Mice were euthanized on day 21. The daily dose and the study protocol were chosen based on previous results showing physiologic effects at these levels^{23,44}. The experimental design is shown in Figure 1.

Analytical determinants

Serum levels of albumin, creatinine (Cr), Ca, and P were measured with the FUJI DRI-CHEM system (Nx500; FUJIFILM, Tokyo Japan). Serum FGF23 was measured with an Intact FGF23 Assay Kit (Kainos, Tokyo, Japan). Systolic blood pressure (sBP) was measured weekly using a tail-cuff system (Softron BP98A; Softron, Tokyo, Japan). Transthoracic echocardiography was performed at the end of the 21-day DOCA treatment period to assess structure and diastolic function. Further details are given in the Supplemental Methods.

Histological analysis

The LV was fixed in 10% formalin overnight, embedded in paraffin, cut into 4- μm thick coronal sections, and stained with hematoxylin and eosin (HE) and Masson-Trichrome stain. The cardiac sections were semi-quantified using an Olympus BX51 microscope coupled to a digital camera and an image analysis system (WinROOF ver. 5.7). Semi-quantification of cardiac fibrosis and hypertrophy (diameter of the myocytes) was performed as previously reported⁴⁵.

For immunohistochemistry, the sections were deparaffinized, rehydrated, and microwaved in 0.01 mol/L citrate buffer (pH 6.0) for 10 min to retrieve antigens. The sections were then treated with 0.6% hydrogen peroxide in methanol for 10 min at room temperature to block endogenous peroxidase and subsequently blocked with 10% pre-immune goat serum for 30 min at room

temperature. A primary rabbit anti-Cyp27b1 antibody (Santa Cruz Biotechnology, Inc. Santa Cruz, CA, USA, 1:200 dilution), rabbit anti-Cyp27a1 antibody (Santa Cruz Biotechnology, 1:100 dilution), or pre-immune IgG was added, followed by incubation at room temperature for 2 h. A biotinylated secondary antibody was then applied, followed by a streptavidin-HRP conjugate. Immune complexes were visualized with 3-amino 9-ethylcarbazole substrate-chromagen. Finally, all sections were counterstained with hematoxylin. Semi-quantification of the positive area was performed in the same manner as that described for cardiac fibrosis⁴⁵.

Quantitative real-time reverse transcription polymerase chain reaction (qRT-PCR)

Total RNA from the LV was extracted using TRIzol reagent (Invitrogen, Carlsbad, CA, USA) according to the manufacturer's instructions. The synthesized cDNA was amplified with a standard PCR protocol using Universal SYBR Green SuperMix (BioRad, Hercules, CA, USA) and mouse-specific primers. Parallel amplification with primers for glyceraldehyde-3-phosphate dehydrogenase (GAPDH) was performed. Mouse-specific primers for FGF23, atrial natriuretic peptide (ANP), brain natriuretic peptide (BNP), collagen type I (COL I), collagen type III (COL III), and GAPDH were purchased from Qiagen (Qiagen K.K, Tokyo, Japan). The cycling conditions were 10 min of preincubation at 95°C, 15 s of denaturation at 95°C, and 1 min of annealing at 60°C for 40 cycles, using a CFX96 Touch Real-Time PCR Detection System (BioRad). The amounts of each transcript were normalized relative to the amount of GAPDH mRNA in each sample. All measurements were performed in duplicate.

Western blot analysis

Protein expression levels of TGF β , total Smad2/3 (tSmad2/3), and phosphorylated Smad2/3 (pSmad2/3) were determined by Western blot analysis. The LV was homogenized in 2 ml of Cell Lysis Buffer (Cell Signaling Technology, Beverly, MA, USA) and samples were centrifuged at 3000 g for 15 min. Supernatants were mixed with SDS-PAGE sample buffer and boiled for 5 min, and samples (10 μ g per lane) were then electrophoresed on 4-12% SDS polyacrylamide gels and transferred to nitrocellulose membranes for 2 h at 30 V. Membranes were blocked for 30 min with Tris-buffered saline containing 5% BSA (5% BSA/TBS) and then incubated with the following diluted primary antibodies overnight at room temperature in 5% BSA/TBS containing 0.05% Tween 20: rabbit anti-TGF β (Cell Signaling Technology; 1:200), anti-Smad2/3 (Cell Signaling Technology; 1:500) and anti-pSmad2/3 (Thermo Fisher Scientific, Waltham, MO; 1:200) or rabbit anti-GAPDH (Cell Signaling Technology; 1:2000). The membranes were washed before addition of diluted horseradish peroxidase (HRP)-conjugated anti-rabbit IgG-HRP or anti-mouse IgG-HRP (Santa Cruz Biotechnology) secondary antibodies. The membranes were rewashed and developed using an enhanced chemiluminescence system (ECL Prime Western Blotting Detection Reagent; GE Healthcare UK, Little Chalfont, Buckinghamshire, UK). Relative protein levels were normalized using the densitometric intensity of GAPDH⁴⁶.

Statistical analysis

Data for each group are expressed as mean \pm standard error of the mean (SEM). Comparisons among experimental groups were performed using one-way ANOVA and Tukey's *post hoc* test for variables showing a normal distribution, and Kruskal-Wallis test followed by Dunn's *post hoc* test for those with a non-normal distribution. Spearman rank correlation analysis was used to test

associations between two parameters. $P < 0.05$ was taken to indicate statistical significance. All analyses were performed with JMP® ver. 11.0 (SAS Institute Inc., Cary, NC, USA).

Results

Effects of intravenous FGF23 loading on serum chemistry

The serum chemistries and physical parameters of each group are shown in Table 1. The serum Cr and Ca levels were similar among the four groups. Serum P was significantly lower in group F (5.2 ± 0.3 mg/dL; $P < 0.05$) than in group V (7.0 ± 0.5 mg/dL). Serum FGF23 was slightly higher in group V (249 ± 30 pg/mL) than in group NC (51 ± 24 pg/mL) and this increase was further amplified in groups F (1416 ± 459 pg/mL; $P < 0.05$ vs. V) and C (1261 ± 85 ; $P < 0.05$ vs. V). Body weight (BW) was similar in the four groups. Heart weight-to-BW (HW/BW) ratio and LVW (left ventricular weight)/BW ratio were significantly higher in group V (HW/BW: 6.9 ± 0.4 , $P < 0.01$; LVW/BW: 4.8 ± 0.2 , $P < 0.01$) and group F (HW/BW: 6.8 ± 0.5 , $P < 0.05$; LVW/BW: 4.8 ± 0.2 , $P < 0.01$) compared to those in group NC (HW/BW: 4.8 ± 0.3 ; LVW/BW: 3.3 ± 0.2). In contrast, these parameters in group C (HW/BW: 5.9 ± 0.4 ; LVW/BW: 4.1 ± 0.5) were similar to those in group NC.

Effects of intravenous FGF23 loading on cardiac function and sBP

Echocardiography by the M-mode of the parasternal long-axis revealed that each group of DOCA-salt mice (groups V, F, and C) showed a similar cardiac size trend. However, LVEF in group F (52 ± 1 %) was lower than that in NC group (61 ± 2 %). LVEF in group C (57 ± 1 %) was similar to those in groups V (56 ± 1 %) and NC (Table 1 and Figure 2A). Doppler echocardiography showed that the early-to-atrial wave ratio (E/A) in group V (1.0 ± 0.2 , $P < 0.05$) was significantly lower than that in group NC (1.9 ± 0.2). E/A was also significantly lower in group F (0.7 ± 0.1 ; $P < 0.01$) compared to that in group NC (1.9 ± 0.2), whereas E/A in group C (2.0 ± 0.3 ; $P < 0.05$ vs V and $P < 0.01$ vs. F) was significantly higher than that in groups V (1.0 ± 0.2) and F (0.7 ± 0.1) (Table 1 and

Figure 2B). sBP in groups V (126 ± 2 mmHg; $P < 0.01$), F (127 ± 1 mmHg; $P < 0.01$), and C (123 ± 5 mmHg; $P < 0.01$) were equally and significantly higher than that in group NC (91 ± 4 mmHg) (Figure 2C).

Cardiac hypertrophy and fibrosis in mice with HFpEF

Cardiac fibrosis was determined by Masson-Trichrome staining (Figure 3A). In semiquantitative analysis, the cardiac fibrosis area was significantly higher in group F (13.2 %; $P < 0.05$) compared with group V (7.0%), and the fibrosis area in group C (3.8%; $P < 0.01$) was significantly lower than that in group F (Figure 3B). Cardiac mRNA levels of COL I and COL III, which are markers of cardiac fibrosis, showed a similar trend (Supplemental Figure 1A, 1B). The average myocardial cell diameter was significantly greater in groups V ($0.27 \mu\text{m}$; $P < 0.01$), F ($0.26 \mu\text{m}$; $P < 0.01$), and C ($0.23 \mu\text{m}$; $P < 0.05$) compared with group NC ($0.17 \mu\text{m}$) (Figure 3C). Cardiac mRNA levels of ANP and BNP, which are markers of LVH, showed a similar trend (Supplemental Figure 1C, 1D), but those of FGF23 were comparable among groups V, F, and C (Supplement Figure 1E).

Cyp27b1 and Cyp24a1 expression in cardiac tissue

Protein expression for Cyp27b1 and Cyp24a1 in cardiac tissue was determined by immunohistochemistry (Figure 4A and B). Semiquantitative analysis showed that the Cyp27b1 area was slightly lower in group V ($25.5 \pm 3.4\%$) than in group NC ($30.3 \pm 2.5\%$), and significantly lower in group F ($14.5 \pm 3.9\%$; $P < 0.01$) than in group V. On the other hand, this decrease in Cyp27b1 was partly reversed in group C ($31.5 \pm 3.0\%$, $P < 0.01$) (Figure 4C). The Cyp24a1 area was significantly lower in group V ($18.8 \pm 5.3\%$; $P < 0.05$) than in group NC ($30.0 \pm 2.2\%$), and significantly higher in

group F ($31.0 \pm 6.9\%$, $P < 0.05$) compared to group V (Figure 4D).

Association of Cyp27b1 and Cyp24a1 expression with cardiac fibrosis

Association of Cyp27b1 and Cyp24a1 with cardiac fibrosis was determined by linear regression analysis. Expression levels of COL I mRNA ($r = 0.63$, $P < 0.01$) and COL III mRNA ($r = 0.69$, $P < 0.01$) were positively correlated with cardiac fibrosis (Supplement Figure 2A, 2B). Cyp27b1 ($r = -0.79$, $P < 0.01$) showed a significant inverse correlation with the cardiac fibrosis area (Figure 5A), but Cyp24a1 ($r = 0.24$, $P = 0.377$) did not show a significant correlation (Figure 5B).

Modification of TGF β /Smad signaling in FGF23-loaded cardiac tissue by calcitriol

Protein expression levels of TGF β , Smad2/3, and phosphorylated Smad2/3 were evaluated by western blotting (Figure 6A). TGF β was significantly higher in group F (1.32-fold to NC; $P < 0.01$) than in group NC, and significantly lower in group C (0.96-fold to NC; $P < 0.05$) than in group F (Figure 6B). Smad 2/3 was significantly higher in group V (2.1-fold to NC; $P < 0.01$) than in group NC, and this increase was further amplified in group F (3.0-fold to NC; $P < 0.01$), whereas the level in group C (1.0-fold to NC; $P < 0.01$) was significantly lower than that in group F (Figure 6C). Phosphorylated Smad2/3 was significantly higher in group V (4.6-fold to NC; $P < 0.01$) and group F (5.3-fold to NC; $P < 0.01$) than in group NC, whereas the level was significantly lower in group C (0.8-fold to NC) compared to those in groups V ($P < 0.01$) and F ($P < 0.01$) (Figure 6D). The phosphorylated Smad2/3 to Smad 2/3 ratio was significantly higher in group V (2.3-fold to NC; $P < 0.01$) and group F (1.8-fold to NC; $P < 0.05$) than in group NC, whereas the level was significantly lower in group C (0.8-fold NC) compared to that in groups V ($P < 0.01$) and F ($P < 0.01$) (Figure

6E).

Discussion

This study showed that CIV FGF23 loading exacerbates cardiac diastolic dysfunction and fibrosis in DOCA-salt mice with concomitant HFpEF^{35,47}. The results also showed that FGF23 loading impaired VD metabolism in cardiac tissue and that cardiac Cyp27b1 levels were inversely correlated with cardiac fibrosis. Calcitriol attenuated this FGF23-induced exacerbation of HFpEF by inhibition of TGF β signaling, and this effect was independent of systemic and local FGF23 levels.

FGF23 has a low affinity for FGF receptors (FGFRs) and generally requires Klotho to form a FGFR-Klotho complex as a co-receptor⁴⁸. However, of the four FGFR isoforms, only FGFR1 can form a co-receptor with Klotho, and thus, FGF23 binds to the other isoforms in a Klotho-independent manner⁴⁹. FGF23 has been shown to induce LVH independently of Klotho by activation of FGFR4 and subsequent calcineurin/nuclear factor of activated T cells (NFAT) signaling in vitro and in vivo^{23,50}. On the other hand, a mouse model with high intra-cardiac FGF23 synthesis using an adeno-associated virus overexpressing murine FGF23 does not cause LVH, thus supporting the role of Klotho or status of phosphate in the progression of LVH⁵¹. Increasing attention has been focused on the role of FGF23 in LVH.

A recent study showed that FGF23 might activate FGFR1 and subsequently the phospholipase C/inositol 1,4,5-trisphosphate signaling pathway, thus leading to the upregulation of calcium release-activated calcium channel protein 1 and/or transient receptor potential canonical 1-mediated Ca²⁺ entry, which enhanced human atrial fibroblast activity⁵². Another experimental study demonstrated that FGF23 directly upregulated profibrotic factors COL I, COL III, and TGF β in mouse cardiac fibroblasts⁵³. Furthermore, other studies have shown that FGF23 increases proliferation of neonatal rat cardiac fibroblasts and expression of TGF β , TGF β receptor/Smad complexes, connective tissue

growth factor, and collagen I^{54,55}. Stimulation of the cardiac renin-angiotensin-aldosterone system by FGF23 contributes to cardiac hypertrophy and fibrosis in vitro and in vivo⁵⁵, and Klotho hypomorphic (*kl/kl*) mice develop myocardial fibrosis due to a significant rise in expression of collagen I and TGF β ⁵⁶. TGF β is also responsible for activating the extracellular signal-regulated kinase 1/2 pathway in *kl/kl* mice, which leads to cardiac hypertrophy and fibrosis. Direct damage to the myocardium was found to induce cardiac production of FGF23 in a myocardial infarction mouse model⁵⁷, with local fibroblasts shown to be the main source of FGF23 in the heart, which accelerates fibronectin and collagen I expression⁵⁷. These findings suggest that FGF23 promotes myocardial fibrosis and exacerbates diastolic dysfunction induced by myocardial infarction and ischemia/reperfusion, which is associated with upregulation of active β -catenin and TGF β ⁵³. Recent studies demonstrated that FGF23 could be induced from cardiomyocytes in the rat right ventricle under profibrotic conditions⁵⁸ and showed that FGF23 is not only expressed in cardiac myocytes but also in cardiac fibroblasts and endothelial cells⁵⁹. These results are consistent with those of a study demonstrating that FGF23 induced from cardiac myocytes promoted cardiac fibrosis via the profibrotic crosstalk between cardiac myocytes and fibroblasts⁵⁴. Thus, FGF23 could be involved in cardiac fibrogenesis in a paracrine/autocrine manner. According to these results, the role of FGF23 in cardiac fibrogenesis remains to be clarified.

FGF23 increases sodium renal uptake in a Klotho-dependent manner, producing a volume overload and hypertension and finally leading to development of LVH⁶⁰. In this study, we found that CIV FGF23 loading resulted in alteration of cardiac VD metabolism locally, an increase in cardiac fibrosis, and HFpEF progression, which were independent of systemic and local FGF23 levels.

A noteworthy finding in the current study was that cardiac Cyp27b1 was decreased by FGF23

loading and that the Cyp27b1 levels were inversely correlated with cardiac fibrosis. A previous study suggested that Cyp27b1 gene knockout mice, which have VD deficiency, showed progression of local organ fibrosis³⁴. Thus, alteration of Cyp27b1 in cardiac tissue by FGF23 loading might have a crucial role in the progression of cardiac fibrosis.

Another interesting finding in this study was that calcitriol slightly ameliorated LVH with marked inhibition of cardiac fibrosis. Activation of TGF β signaling has been shown to be associated with production and deposition of extracellular matrix protein, including collagen and fibronectin, in cardiac tissue⁶¹. Transgenic mice overexpressing TGF β exhibit cardiac hypertrophy accompanied by cardiac fibrosis⁶², and attenuation of TGF β signaling by an anti-TGF β neutralizing antibody suppressed collagen accumulation following pressure overload⁶³. Calcitriol has been shown to attenuate cardiomyopathy induced by doxorubicin and suppress TGF β -induced Smad2/3 phosphorylation⁶⁴. In addition, supplementation of calcitriol has been found to suppress renal fibrosis mediating VDR, which suppressed TGF β /Smad signal transduction⁶⁵. We found that calcitriol attenuated cardiac fibrosis through blockade of the TGF β /Smad2/3 pathway, which might contribute to suppression of HFpEF progression. This cardioprotective effect of calcitriol was independent of systemic and local FGF23 levels, which could explain the discrepancy between the favorable association of VD derivatives with cardiovascular outcomes^{66,67} and the increase in FGF23 due to administration of these derivatives in CKD⁶⁸.

The study has several limitations. First, we did not investigate the optimal dosage of calcitriol for maximizing cardioprotective effects. Second, we could not measure serum calcitriol levels because of a lack of serum samples. Since a previous study showed that injection of recombinant FGF-23 reduced serum calcitriol⁶⁹, a decrease in serum calcitriol is expected in our model. Also, calcitriol

administration could increase serum calcitriol levels, and may have ameliorated cardiac impairment due to attenuation of TGF β signaling. We focused on the change in local VD metabolism in this study, and the effects of systemic calcitriol levels on cardiac alterations remain to be studied. Third, our study has a small sample size; however, the reliability of the results is preserved because of the small variability.

In conclusion, CIV FGF23 loading induced cardiac fibrosis concomitantly with locally abnormal vitamin D metabolism, and this might have contributed to HFpEF progression in the DOCA-salt mouse model. Thus, cardiac toxicity of FGF23 may be partly due to VD inactivation in cardiac tissue. Calcitriol has cardioprotective effects by mediating TGF β signaling, independently of local and systemic FGF23 levels.

Author Contributions

T.S. and M.M. conceived and designed the study; T.S., M.M., and T.K. performed experiments; H.O., F.K., and H.H. analyzed data; T.S. and M.M. interpreted the results; T.S. prepared figures; T.S., M.M., H.O., F.K., and H.H. drafted the manuscript; T.S., M.M., H.O., F.K., and H.H. edited and revised the manuscript; All authors read and approved the final version of manuscript.

Competing Interests

The authors declare that they have no competing interests.

Funding

The study was partly supported by a grant from the Japanese Association of Dialysis Physicians (No. 2018-1).

Data Availability

The datasets used and/or analyzed during the current study are available from the corresponding author on reasonable request.

Ethics Approval and Consent to Participate

This study does not involve human subjects and thus does not require informed consent from patients, which was determined by the Institutional Review Board (IRB) at Showa University School of Medicine. The animal protocol was approved by the institutional animal experiment ethics committee of Showa University.

References

- 1 Go, A. S., Chertow, G. M., Fan, D., McCulloch, C. E. & Hsu, C. Y. Chronic kidney disease and the risks of death, cardiovascular events, and hospitalization. *N Engl J Med* **351**, 1296-1305 (2004).
- 2 Johansen, K. L., Chertow, G. M., Foley, R. N., Gilbertson, D. T., Herzog, C. A., Ishani, A. *et al.* US Renal Data System 2020 Annual Data Report: Epidemiology of Kidney Disease in the United States. *Am J Kidney Dis* **77**, A7-a8 (2021).
- 3 Foley, R. N., Parfrey, P. S., Harnett, J. D., Kent, G. M., Martin, C. J., Murray, D. C. *et al.* Clinical and echocardiographic disease in patients starting end-stage renal disease therapy. *Kidney Int* **47**, 186-192 (1995).
- 4 Yancy, C. W., Lopatin, M., Stevenson, L. W., De Marco, T. & Fonarow, G. C. Clinical presentation, management, and in-hospital outcomes of patients admitted with acute decompensated heart failure with preserved systolic function: a report from the Acute Decompensated Heart Failure National Registry (ADHERE) Database. *J Am Coll Cardiol* **47**, 76-84 (2006).
- 5 Lam, C. S., Donal, E., Kraigher-Krainer, E. & Vasan, R. S. Epidemiology and clinical course of heart failure with preserved ejection fraction. *European journal of heart failure* **13**, 18-28 (2011).
- 6 Ather, S., Chan, W., Bozkurt, B., Aguilar, D., Ramasubbu, K., Zachariah, A. A. *et al.* Impact of noncardiac comorbidities on morbidity and mortality in a predominantly male population with heart failure and preserved versus reduced ejection fraction. *J Am Coll Cardiol* **59**, 998-1005 (2012).

- 7 Brouwers, F. P., de Boer, R. A., van der Harst, P., Voors, A. A., Gansevoort, R. T., Bakker, S. J. *et al.* Incidence and epidemiology of new onset heart failure with preserved vs. reduced ejection fraction in a community-based cohort: 11-year follow-up of PREVEND. *Eur Heart J* **34**, 1424-1431 (2013).
- 8 Laurent, S., Cockcroft, J., Van Bortel, L., Boutouyrie, P., Giannattasio, C., Hayoz, D. *et al.* Expert consensus document on arterial stiffness: methodological issues and clinical applications. *Eur Heart J* **27**, 2588-2605 (2006).
- 9 Briet, M., Boutouyrie, P., Laurent, S. & London, G. M. Arterial stiffness and pulse pressure in CKD and ESRD. *Kidney Int* **82**, 388-400 (2012).
- 10 Foley, R. N., Curtis, B. M., Randell, E. W. & Parfrey, P. S. Left ventricular hypertrophy in new hemodialysis patients without symptomatic cardiac disease. *Clin J Am Soc Nephrol* **5**, 805-813 (2010).
- 11 Brown, N. J. Contribution of aldosterone to cardiovascular and renal inflammation and fibrosis. *Nat Rev Nephrol* **9**, 459-469 (2013).
- 12 Nolte, K., Herrmann-Lingen, C., Platschek, L., Holzendorf, V., Pilz, S., Tomaschitz, A. *et al.* Vitamin D deficiency in patients with diastolic dysfunction or heart failure with preserved ejection fraction. *ESC Heart Fail* **6**, 262-270 (2019).
- 13 Stinghen, A. E., Massy, Z. A., Vlassara, H., Striker, G. E. & Boullier, A. Uremic Toxicity of Advanced Glycation End Products in CKD. *J Am Soc Nephrol* **27**, 354-370 (2016).
- 14 Gutierrez, O., Isakova, T., Rhee, E., Shah, A., Holmes, J., Collerone, G. *et al.* Fibroblast growth factor-23 mitigates hyperphosphatemia but accentuates calcitriol deficiency in chronic kidney disease. *J Am Soc Nephrol* **16**, 2205-2215 (2005).

- 15 Isakova, T., Xie, H., Yang, W., Xie, D., Anderson, A. H., Scialla, J. *et al.* Fibroblast growth factor 23 and risks of mortality and end-stage renal disease in patients with chronic kidney disease. *JAMA* **305**, 2432-2439 (2011).
- 16 Martin, A., David, V. & Quarles, L. D. Regulation and function of the FGF23/klotho endocrine pathways. *Physiol Rev* **92**, 131-155 (2012).
- 17 Memmos, E. & Papagianni, A. New Insights into the Role of FGF-23 and Klotho in Cardiovascular Disease in Chronic Kidney Disease Patients. *Current vascular pharmacology* **19**, 55-62 (2021).
- 18 Quarles, L. D. Role of FGF23 in vitamin D and phosphate metabolism: implications in chronic kidney disease. *Experimental cell research* **318**, 1040-1048 (2012).
- 19 Adams, J. S., Rafison, B., Witzel, S., Reyes, R. E., Shieh, A., Chun, R. *et al.* Regulation of the extrarenal CYP27B1-hydroxylase. *J Steroid Biochem Mol Biol* **144 Pt A**, 22-27 (2014).
- 20 Jones, G. Extrarenal vitamin D activation and interactions between vitamin D₂, vitamin D₃, and vitamin D analogs. *Annual review of nutrition* **33**, 23-44 (2013).
- 21 Sun, W., Chen, L., Zhang, W., Wang, R., Goltzman, D. & Miao, D. Active vitamin D deficiency mediated by extracellular calcium and phosphorus results in male infertility in young mice. *Am J Physiol Endocrinol Metab* **308**, E51-62 (2015).
- 22 Gutierrez, O. M., Januzzi, J. L., Isakova, T., Laliberte, K., Smith, K., Collerone, G. *et al.* Fibroblast growth factor 23 and left ventricular hypertrophy in chronic kidney disease. *Circulation* **119**, 2545-2552 (2009).
- 23 Faul, C., Amaral, A. P., Oskouei, B., Hu, M. C., Sloan, A., Isakova, T. *et al.* FGF23 induces left ventricular hypertrophy. *J Clin Invest* **121**, 4393-4408 (2011).

- 24 Leifheit-Nestler, M. & Haffner, D. Paracrine Effects of FGF23 on the Heart. *Front Endocrinol (Lausanne)* **9**, 278 (2018).
- 25 Haussler, M. R., Whitfield, G. K., Kaneko, I., Haussler, C. A., Hsieh, D., Hsieh, J. C. *et al.* Molecular mechanisms of vitamin D action. *Calcif Tissue Int* **92**, 77-98 (2013).
- 26 Hasegawa, H., Nagano, N., Urakawa, I., Yamazaki, Y., Iijima, K., Fujita, T. *et al.* Direct evidence for a causative role of FGF23 in the abnormal renal phosphate handling and vitamin D metabolism in rats with early-stage chronic kidney disease. *Kidney Int* **78**, 975-980 (2010).
- 27 Gunta, S. S., Thadhani, R. I. & Mak, R. H. The effect of vitamin D status on risk factors for cardiovascular disease. *Nat Rev Nephrol* **9**, 337-347 (2013).
- 28 Shoben, A. B., Rudser, K. D., de Boer, I. H., Young, B. & Kestenbaum, B. Association of oral calcitriol with improved survival in nondialyzed CKD. *J Am Soc Nephrol* **19**, 1613-1619 (2008).
- 29 Teng, M., Wolf, M., Ofsthun, M. N., Lazarus, J. M., Hernan, M. A., Camargo, C. A., Jr. *et al.* Activated injectable vitamin D and hemodialysis survival: a historical cohort study. *J Am Soc Nephrol* **16**, 1115-1125 (2005).
- 30 Thadhani, R., Appelbaum, E., Pritchett, Y., Chang, Y., Wenger, J., Tamez, H. *et al.* Vitamin D therapy and cardiac structure and function in patients with chronic kidney disease: the PRIMO randomized controlled trial. *Jama* **307**, 674-684 (2012).
- 31 Chen, S., Law, C. S., Grigsby, C. L., Olsen, K., Hong, T. T., Zhang, Y. *et al.* Cardiomyocyte-specific deletion of the vitamin D receptor gene results in cardiac hypertrophy. *Circulation* **124**, 1838-1847 (2011).
- 32 Bodyak, N., Ayus, J. C., Achinger, S., Shivalingappa, V., Ke, Q., Chen, Y. S. *et al.* Activated vitamin D attenuates left ventricular abnormalities induced by dietary sodium in Dahl salt-

- sensitive animals. *Proceedings of the National Academy of Sciences of the United States of America* **104**, 16810-16815 (2007).
- 33 Zhang, Z. L., Ding, X. F., Tong, J. & Li, B. Y. Enhanced radiosensitivity in 1,25-dihydroxyvitamin D3 deficient mice. *Journal of radiation research* **52**, 215-219 (2011).
- 34 Li, S. R., Tan, Z. X., Chen, Y. H., Hu, B., Zhang, C., Wang, H. *et al.* Vitamin D deficiency exacerbates bleomycin-induced pulmonary fibrosis partially through aggravating TGF- β /Smad2/3-mediated epithelial-mesenchymal transition. *Respiratory research* **20**, 266 (2019).
- 35 Silberman, G. A., Fan, T. H., Liu, H., Jiao, Z., Xiao, H. D., Lovelock, J. D. *et al.* Uncoupled cardiac nitric oxide synthase mediates diastolic dysfunction. *Circulation* **121**, 519-528 (2010).
- 36 Dornas, W. C. & Silva, M. E. Animal models for the study of arterial hypertension. *Journal of biosciences* **36**, 731-737 (2011).
- 37 Noll, N. A., Lal, H. & Merryman, W. D. Mouse Models of Heart Failure with Preserved or Reduced Ejection Fraction. *The American journal of pathology* **190**, 1596-1608 (2020).
- 38 Lovelock, J. D., Monasky, M. M., Jeong, E. M., Lardin, H. A., Liu, H., Patel, B. G. *et al.* Ranolazine improves cardiac diastolic dysfunction through modulation of myofilament calcium sensitivity. *Circ Res* **110**, 841-850 (2012).
- 39 Sam, F., Duhaney, T. A., Sato, K., Wilson, R. M., Ohashi, K., Sono-Romanelli, S. *et al.* Adiponectin deficiency, diastolic dysfunction, and diastolic heart failure. *Endocrinology* **151**, 322-331 (2010).
- 40 Tanaka, K., Wilson, R. M., Essick, E. E., Duffen, J. L., Scherer, P. E., Ouchi, N. *et al.* Effects of adiponectin on calcium-handling proteins in heart failure with preserved ejection fraction. *Circ Heart Fail* **7**, 976-985 (2014).

- 41 Wilson, R. M., De Silva, D. S., Sato, K., Izumiya, Y. & Sam, F. Effects of fixed-dose isosorbide dinitrate/hydralazine on diastolic function and exercise capacity in hypertension-induced diastolic heart failure. *Hypertension* **54**, 583-590 (2009).
- 42 Grobe, J. L., Buehrer, B. A., Hilzendeger, A. M., Liu, X., Davis, D. R., Xu, D. *et al.* Angiotensinergic signaling in the brain mediates metabolic effects of deoxycorticosterone (DOCA)-salt in C57 mice. *Hypertension* **57**, 600-607 (2011).
- 43 Kandlikar, S. S. & Fink, G. D. Mild DOCA-salt hypertension: sympathetic system and role of renal nerves. *Am J Physiol Heart Circ Physiol* **300**, H1781-1787 (2011).
- 44 Henley, C., Davis, J., Miller, G., Shatzen, E., Cattley, R., Li, X. *et al.* The calcimimetic AMG 641 abrogates parathyroid hyperplasia, bone and vascular calcification abnormalities in uremic rats. *European journal of pharmacology* **616**, 306-313 (2009).
- 45 Mizobuchi, M., Ogata, H., Hosaka, N., Kumata, C., Nakazawa, A., Kondo, F. *et al.* Effects of calcimimetic combined with an angiotensin-converting enzyme inhibitor on uremic cardiomyopathy progression. *Am J Nephrol* **34**, 256-267 (2011).
- 46 Mizobuchi, M., Morrissey, J., Finch, J. L., Martin, D. R., Liapis, H., Akizawa, T. *et al.* Combination therapy with an angiotensin-converting enzyme inhibitor and a vitamin D analog suppresses the progression of renal insufficiency in uremic rats. *J Am Soc Nephrol* **18**, 1796-1806 (2007).
- 47 Schnelle, M., Catibog, N., Zhang, M., Nabeebaccus, A. A., Anderson, G., Richards, D. A. *et al.* Echocardiographic evaluation of diastolic function in mouse models of heart disease. *J Mol Cell Cardiol* **114**, 20-28 (2018).
- 48 Yu, X., Ibrahimi, O. A., Goetz, R., Zhang, F., Davis, S. I., Garringer, H. J. *et al.* Analysis of the

- biochemical mechanisms for the endocrine actions of fibroblast growth factor-23. *Endocrinology* **146**, 4647-4656 (2005).
- 49 Urakawa, I., Yamazaki, Y., Shimada, T., Iijima, K., Hasegawa, H., Okawa, K. *et al.* Klotho converts canonical FGF receptor into a specific receptor for FGF23. *Nature* **444**, 770-774 (2006).
- 50 Grabner, A., Amaral, A. P., Schramm, K., Singh, S., Sloan, A., Yanucil, C. *et al.* Activation of Cardiac Fibroblast Growth Factor Receptor 4 Causes Left Ventricular Hypertrophy. *Cell Metab* **22**, 1020-1032 (2015).
- 51 Leifheit-Nestler, M., Wagner, M. A., Richter, B., Piepert, C., Eitner, F., Böckmann, I. *et al.* Cardiac Fibroblast Growth Factor 23 Excess Does Not Induce Left Ventricular Hypertrophy in Healthy Mice. *Frontiers in cell and developmental biology* **9**, 745892 (2021).
- 52 Lee, T. W., Chung, C. C., Lee, T. I., Lin, Y. K., Kao, Y. H. & Chen, Y. J. Fibroblast Growth Factor 23 Stimulates Cardiac Fibroblast Activity through Phospholipase C-Mediated Calcium Signaling. *Int J Mol Sci* **23** (2021).
- 53 Hao, H., Li, X., Li, Q., Lin, H., Chen, Z., Xie, J. *et al.* FGF23 promotes myocardial fibrosis in mice through activation of β -catenin. *Oncotarget* **7**, 64649-64664 (2016).
- 54 Leifheit-Nestler, M., Kirchhoff, F., Nespore, J., Richter, B., Soetje, B., Klintschar, M. *et al.* Fibroblast growth factor 23 is induced by an activated renin-angiotensin-aldosterone system in cardiac myocytes and promotes the pro-fibrotic crosstalk between cardiac myocytes and fibroblasts. *Nephrol Dial Transplant* **33**, 1722-1734 (2018).
- 55 Bockmann, I., Lischka, J., Richter, B., Deppe, J., Rahn, A., Fischer, D. C. *et al.* FGF23-Mediated Activation of Local RAAS Promotes Cardiac Hypertrophy and Fibrosis. *Int J Mol*

Sci **20** (2019).

- 56 Leifheit-Nestler, M., Richter, B., Basaran, M., Nespor, J., Vogt, I., Alesutan, I. *et al.* Impact of Altered Mineral Metabolism on Pathological Cardiac Remodeling in Elevated Fibroblast Growth Factor 23. *Front Endocrinol (Lausanne)* **9**, 333 (2018).
- 57 Schumacher, D., Alampour-Rajabi, S., Ponomariov, V., Curaj, A., Wu, Z., Staudt, M. *et al.* Cardiac FGF23: new insights into the role and function of FGF23 after acute myocardial infarction. *Cardiovascular pathology : the official journal of the Society for Cardiovascular Pathology* **40**, 47-54 (2019).
- 58 Kuga, K., Kusakari, Y., Uesugi, K., Semba, K., Urashima, T., Akaike, T. *et al.* Fibrosis growth factor 23 is a promoting factor for cardiac fibrosis in the presence of transforming growth factor- β 1. *PLoS One* **15**, e0231905 (2020).
- 59 Eitner, F., Richter, B., Schwänen, S., Szaroszyk, M., Vogt, I., Grund, A. *et al.* Comprehensive Expression Analysis of Cardiac Fibroblast Growth Factor 23 in Health and Pressure-induced Cardiac Hypertrophy. *Frontiers in cell and developmental biology* **9**, 791479 (2021).
- 60 Andrukhova, O., Slavic, S., Smorodchenko, A., Zeitz, U., Shalhoub, V., Lanske, B. *et al.* FGF23 regulates renal sodium handling and blood pressure. *EMBO molecular medicine* **6**, 744-759 (2014).
- 61 MacKenna, D., Summerour, S. R. & Villarreal, F. J. Role of mechanical factors in modulating cardiac fibroblast function and extracellular matrix synthesis. *Cardiovasc Res* **46**, 257-263 (2000).
- 62 Rosenkranz, S., Flesch, M., Amann, K., Haeuseler, C., Kilter, H., Seeland, U. *et al.* Alterations of beta-adrenergic signaling and cardiac hypertrophy in transgenic mice overexpressing TGF-

beta(1). *Am J Physiol Heart Circ Physiol* **283**, H1253-1262 (2002).

- 63 Kuwahara, F., Kai, H., Tokuda, K., Kai, M., Takeshita, A., Egashira, K. *et al.* Transforming growth factor-beta function blocking prevents myocardial fibrosis and diastolic dysfunction in pressure-overloaded rats. *Circulation* **106**, 130-135 (2002).
- 64 Tsai, T. H., Lin, C. J., Hang, C. L. & Chen, W. Y. Calcitriol Attenuates Doxorubicin-Induced Cardiac Dysfunction and Inhibits Endothelial-to-Mesenchymal Transition in Mice. *Cells* **8** (2019).
- 65 Ito, I., Waku, T., Aoki, M., Abe, R., Nagai, Y., Watanabe, T. *et al.* A nonclassical vitamin D receptor pathway suppresses renal fibrosis. *J Clin Invest* **123**, 4579-4594 (2013).
- 66 Lu, R. J., Zhu, S. M., Tang, F. L., Zhu, X. S., Fan, Z. D., Wang, G. L. *et al.* Effects of vitamin D or its analogues on the mortality of patients with chronic kidney disease: an updated systematic review and meta-analysis. *European journal of clinical nutrition* **71**, 683-693 (2017).
- 67 Zittermann, A., Trummer, C., Theiler-Schwetz, V., Lerchbaum, E., März, W. & Pilz, S. Vitamin D and Cardiovascular Disease: An Updated Narrative Review. *Int J Mol Sci* **22** (2021).
- 68 Vervloet, M. G., Sezer, S., Massy, Z. A., Johansson, L., Cozzolino, M. & Fouque, D. The role of phosphate in kidney disease. *Nat Rev Nephrol* **13**, 27-38 (2017).
- 69 Shimada, T., Hasegawa, H., Yamazaki, Y., Muto, T., Hino, R., Takeuchi, Y. *et al.* FGF-23 is a potent regulator of vitamin D metabolism and phosphate homeostasis. *J Bone Miner Res* **19**, 429-435 (2004).

Figure Legends

Figure 1. Experimental design and group distribution. Wild type male mice were allocated randomly to four groups (n = 4 per group): NC, V, F, and C. DOCA-salt mice were anesthetized and received DOCA from subcutaneous pellets (50 mg/pellet) and nephrectomy of the left kidney. One week after the operation, these mice were fitted with an infusion mini-pump (iPRECIO® model SMP-300, Primetech Corp., Tokyo, Japan) (day 7). Experiments were initiated 5 days after this operation to allow time for recovery. Then, group V was infused with vehicle, group F with FGF23 (80 µg/kg/day), and group C with FGF23 (80 µg/kg/day) and calcitriol (0.4 µg/kg/day ip three times per week) (day 12). Blood pressure was measured weekly. Mice were examined by echocardiography and euthanized after treatment for 10 days (day 21). Abbreviations: NC, normal control; DOCA, deoxycorticosterone acetate; FGF23, fibroblast growth factor 23; BP, blood pressure.

Figure 2. Effect of FGF23 on transthoracic echocardiography and blood pressure after DOCA-salt treatment. (A) M-mode echocardiography of the left ventricular chamber. Group V showed a slightly reduced ejection fraction (EF), whereas EF was maintained in groups F and C. (B) Doppler flow measurement of mitral inflow velocity. DOCA-salt treatment induced a reduction in E/A ratio. (C) sBP measured using a mouse tail-cuff system before and after DOCA-salt treatment. ^{##} P < 0.01 vs. NC, [#] P < 0.05 vs. NC. Abbreviations: NC, normal control; V, vehicle-treated deoxycorticosterone acetate (DOCA)-salt mice; F, FGF23-treated DOCA-salt mice; C, FGF23 and calcitriol-treated DOCA-salt mice; FGF23, fibroblast growth factor 23; IVSd, interventricular septal end diastole; IVSs, interventricular septal end systole; LVIDd, left ventricular (LV) internal diameter end diastole; LVIDs, LV internal diameter end systole; LVPWd, LV posterior wall end diastole; LVPWs, LV

posterior wall end systole, sBP: systolic blood pressure.

Figure 3. Representative microphotographs of cardiac fibrosis and hypertrophy. (A) Sections were deparaffinized and subjected to Masson trichrome staining for collagen. Myocardial fibers and collagen are colored blue. Scale bar = 100 μ m. Magnification at 100x. Inset is magnified microphotograph (200x) of each section. (B) Semiquantitative analysis of cardiac fibrosis. (C) Average myocardial cell diameter based on hematoxylin and eosin staining. Results are shown as mean \pm SEM (n = 4 per group). ** P < 0.01 vs. F, $^{\$}$ P < 0.05 vs. F, $^{##}$ P < 0.01 vs. NC, $^{\#}$ P < 0.05 vs. NC.

Abbreviations: NC, normal control; V, vehicle-treated deoxycorticosterone acetate (DOCA)-salt mice; F, FGF23-treated DOCA-salt mice; C, FGF23 and calcitriol-treated DOCA-salt mice; FGF23, fibroblast growth factor 23.

Figure 4. Cyp27b1 and Cyp24a1 expression in cardiac tissue. Immunohistochemistry of (A) Cyp27b1 and (B) Cyp24a1. Localization of (C) Cyp27b1 and (D) Cyp24a1 was evaluated by semiquantitative analysis. Results are shown as mean \pm SEM (n = 4 per group). Scale bar = 50 μ m. Magnification at 200x. ** P < 0.01 vs. F, $^{\$}$ P < 0.05 vs. F, $^{\#}$ P < 0.05 vs. NC. Abbreviations: NC, normal control; V, vehicle-treated deoxycorticosterone acetate (DOCA)-salt mice; F, FGF23-treated DOCA-salt mice; C, FGF23 and calcitriol-treated DOCA-salt mice; FGF23, fibroblast growth factor 23; Cyp, cytochrome P450.

Figure 5. Correlations of cardiac fibrosis with Cyp27b1 and Cyp24a1 levels. (A) Cyp27b1 and (B)

Cyp24a1 compared with cardiac fibrosis quantification. Abbreviation: Cyp, cytochrome P450.

Figure 6. TGF β /Smad signaling pathway in cardiac tissue. (A) Representative immunoblotting analyses of pSmad2/3, Smad2/3, and TGF β . GAPDH was used as an internal control. Densitometric quantification of the corresponding bands was performed using an image analyzer: (B) TGF, (C) Smad2/3, (D) pSmad2/3, and (E) pSmad2/3 to Smad2/3 ratio. Quantification of relative protein levels. The results are shown as mean \pm SEM (n = 3 per group). ^{\$\$}P < 0.01 vs. F, ^{\$}P < 0.05 vs. F, ^{**}P < 0.01 vs. V. Abbreviations: NC, normal control; V, vehicle-treated deoxycorticosterone acetate (DOCA)-salt mice; F, FGF23-treated DOCA-salt mice; C, FGF23 and calcitriol-treated DOCA-salt mice; FGF23, fibroblast growth factor 23; TGF β , transforming growth factor β ; pSmad2/3, phosphorylated Smad2/3.

Summary of the manuscript

We studied the effect of continuous intravenous (CIV) fibroblast growth factor 23 (FGF23) loading in a deoxycorticosterone acetate-salt mouse model with mild chronic kidney disease, hypertension, and heart failure with a preserved ejection fraction. Our results suggest that CIV FGF23 loading exacerbates cardiac fibrosis and locally abnormal vitamin D metabolism might be involved in this mechanism. Calcitriol attenuates this exacerbation by mediating transforming growth factor β signaling, independent of the FGF23 level.

Supplemental methods

Echocardiography: Transthoracic echocardiography was performed at the end of the 21-day DOCA treatment period using a SonoScape S6V® equipped with a high-frequency ultrasound probe (Shoei Japan Co., Ltd, Osaka, Japan). Mice were anesthetized using 0.5–1.5% isoflurane. [1] The maximum of 1.5% isoflurane has minimal effects on diastolic function. Images were recorded for 30–40 cardiac cycles and measurements were made from 3–5 representative cycles. Interventricular septal end diastole (IVSd), interventricular septal end systole (IVSs), LV internal diameter end diastole (LVIDd), LV internal diameter end systole (LVIDs), LV posterior wall end diastole (LVPWd), LV posterior wall end systole (LVPWs), and LV ejection fraction (LVEF) were measured digitally on M-mode tracings and averaged from at least 3 separate cardiac cycles: LVEF (%) = $100 \times [(LV \text{ Vold} - LV \text{ Vols}) / LV \text{ Vold}]$; LV Vold (μl) = $7.0 / (2.4 + LVIDd) \times LVIDd^3$; LV Vols (μl) = $7.0 / (2.4 + LVIDs) \times LVIDs^3$. Doppler echocardiographic measurement of mitral inflow velocity was used to evaluate cardiac diastolic function. Mitral valve early (E) wave peak, atrial (A) wave peak, and E wave deceleration time (DT) were measured. The transmitral ratio of the peak E to peak A wave velocities (E/A) was normalized to each R-wave and R-wave interval, and expressed as a percentage of the cardiac cycle.

Supplemental Reference

1. Zhou YQ, Foster FS, Parkes R, *et al.* Developmental changes in left and right ventricular diastolic filling patterns in mice. *Am J Physiol Heart Circ Physiol* 2003;285(4):H1563-1575

Supplemental Material of Contents

Supplemental Figure 1. mRNA levels of markers of hypertrophy and fibrosis and of FGF23 in cardiac tissue. Markers of cardiac hypertrophy and fibrosis were determined by qRT-PCR analysis of (A) COL I, (B) COL III, (C) ANP, (D) BNP. (E) FGF23 mRNA expression in cardiac tissue. Results are shown as mean \pm SEM (n = 4 per group). ^{\$} P < 0.05 vs. F, [#] P < 0.05 vs. NC. Abbreviations: NC, normal control; V, vehicle-treated deoxycorticosterone acetate (DOCA)-salt mice; F, FGF23-treated DOCA-salt mice; C, FGF23 and calcitriol-treated DOCA-salt mice; FGF23, fibroblast growth factor 23, COL I, collagen type I; COL III, collagen type III; ANP, atrial natriuretic peptide; BNP, brain natriuretic peptide.

Supplemental Figure 2. Correlations of cardiac fibrosis with mRNA levels of (A) COL I and (B) COL III. Abbreviations: COL I, collagen type I; COL III, collagen type III.

Table 1. Characteristics of each group.

Parameters	NC	V	F	C
Cr, mg/dL	0.2 ± 0.0	0.2 ± 0.0	0.2 ± 0.1	0.4 ± 0.1
Ca, mg/dL	7.3 ± 0.6	7.8 ± 0.4	7.0 ± 0.5	8.7 ± 0.3
P, mg/dL	5.5 ± 0.3	7.0 ± 0.5	5.2 ± 0.3 ^c	5.3 ± 0.5
Intact FGF23, pg/mL	51 ± 24	249 ± 30	1416 ± 459 ^{b,c}	1261 ± 85 ^{a,c}
Weight				
BW, g	24.9 ± 0.5	23.3 ± 0.5	23.1 ± 0.5	24.5 ± 0.5
HW, mg	120.0 ± 8.7	160.0 ± 8.7	155.0 ± 8.7	145.8 ± 8.7
HW/BW	4.8 ± 0.3	6.9 ± 0.4 ^b	6.8 ± 0.5 ^a	5.9 ± 0.4
LVW/BW	3.3 ± 0.2	4.8 ± 0.2 ^b	4.8 ± 0.2 ^b	4.1 ± 0.5
sBP, mmHg	91 ± 4	126 ± 2 ^b	127 ± 1 ^b	123 ± 5 ^b
Left ventricle structure				
IVSd (mm)	0.10 ± 0.03	0.09 ± 0.03	0.08 ± 0.02	0.08 ± 0.02
IVSs (mm)	0.12 ± 0.03	0.12 ± 0.03	0.09 ± 0.01	0.09 ± 0.01
LVIDd (mm)	0.30 ± 0.05	0.34 ± 0.06	0.37 ± 0.09	0.30 ± 0.03
LVIDs (mm)	0.22 ± 0.03	0.26 ± 0.05	0.29 ± 0.07	0.23 ± 0.02
LVPWd (mm)	0.10 ± 0.04	0.11 ± 0.02	0.09 ± 0.03	0.10 ± 0.01
LVPWs (mm)	0.10 ± 0.04	0.11 ± 0.03	0.12 ± 0.06	0.10 ± 0.01
LVEF, %	61 ± 2	56 ± 1	52 ± 1 ^a	57 ± 1
Diastolic function				
E/A	1.9 ± 0.2	1.0 ± 0.2 ^a	0.7 ± 0.1 ^b	2.0 ± 0.3 ^{c,d}

Data are presented as the means ± SEM: n = 4 per group. ^aP < 0.05 vs. NC, ^bP < 0.01 vs. NC, ^cP <

0.05 vs. V, and ^dP < 0.01 vs. F. Abbreviations: NC, normal control; V, vehicle-treated

deoxycorticosterone acetate (DOCA)-salt mice; F, FGF23-treated DOCA-salt mice; C, FGF23 and

calcitriol-treated DOCA-salt mice; Cr, serum creatinine; Ca, calcium; P, serum phosphate; FGF 23,

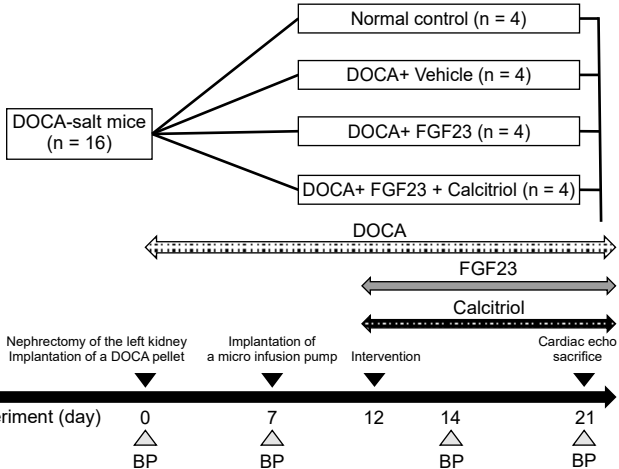
fibroblast growth factor 23; BW, body weight; HW, heart weight; LVW, left ventricular weight; sBP,

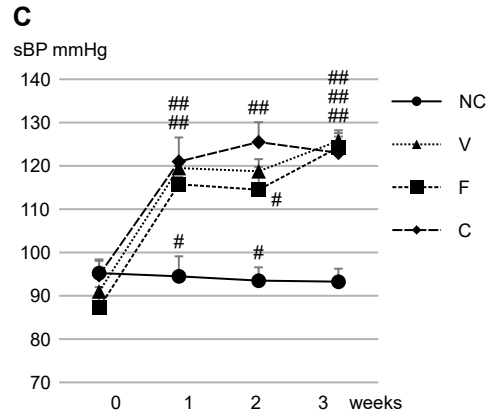
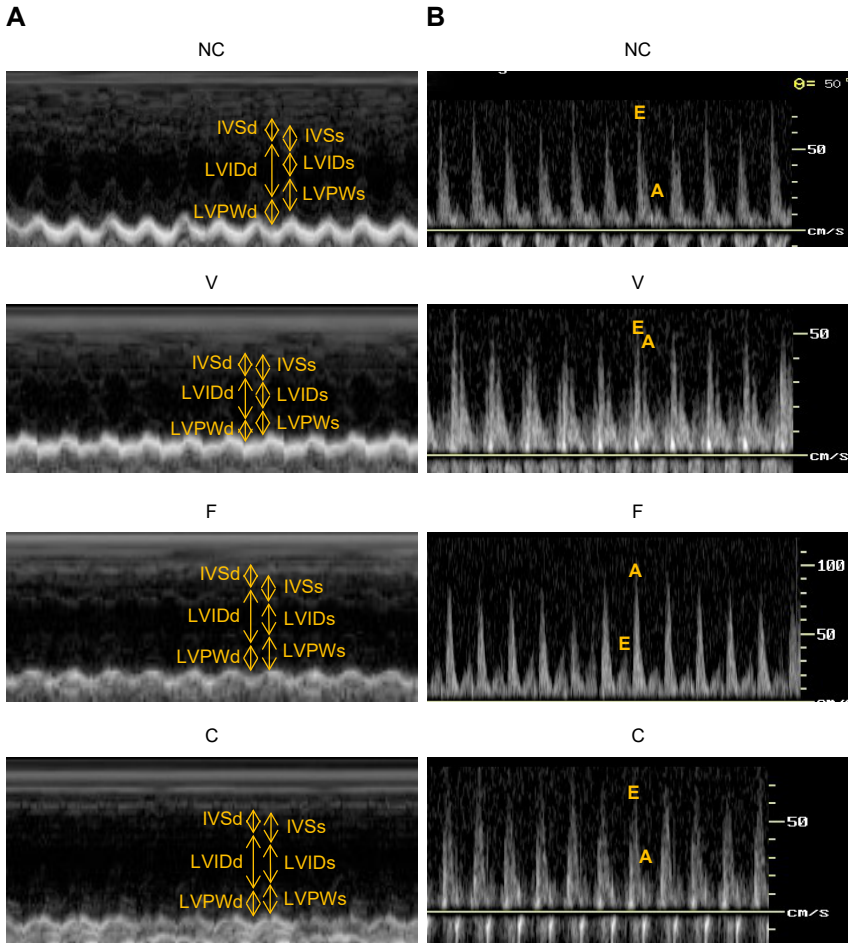
systolic blood pressure; IVSd, interventricular septal end diastole; IVSs, interventricular septal end

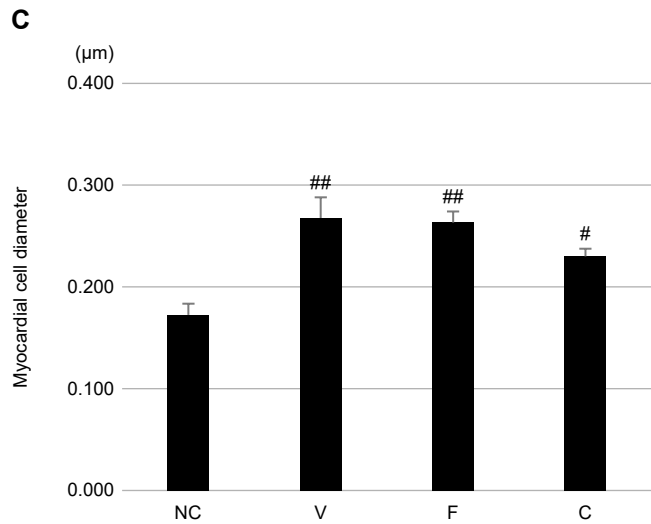
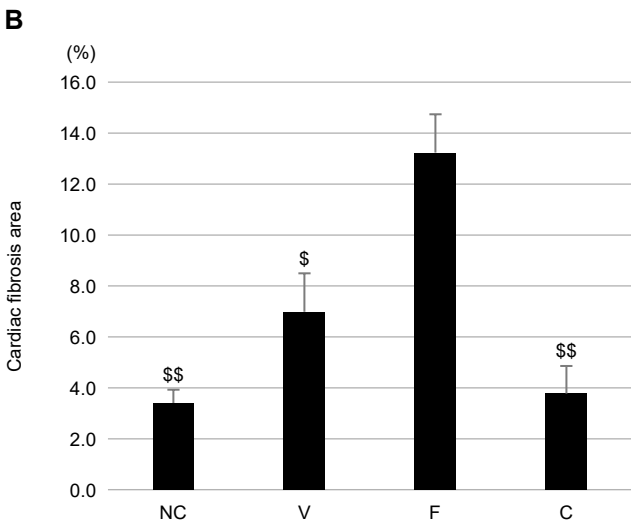
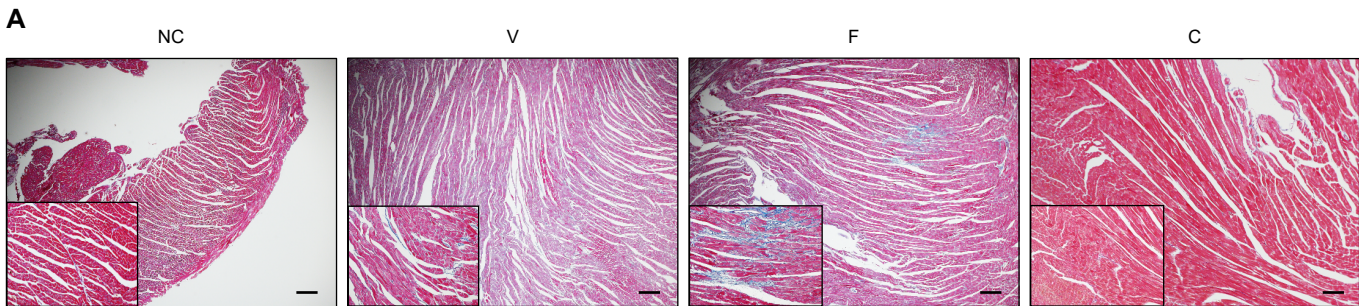
systole; LVIDd, left ventricular (LV) internal diameter end diastole; LVIDs, LV internal diameter end

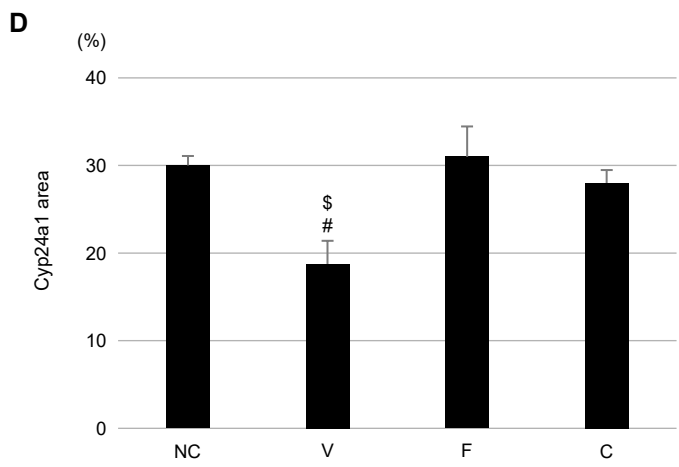
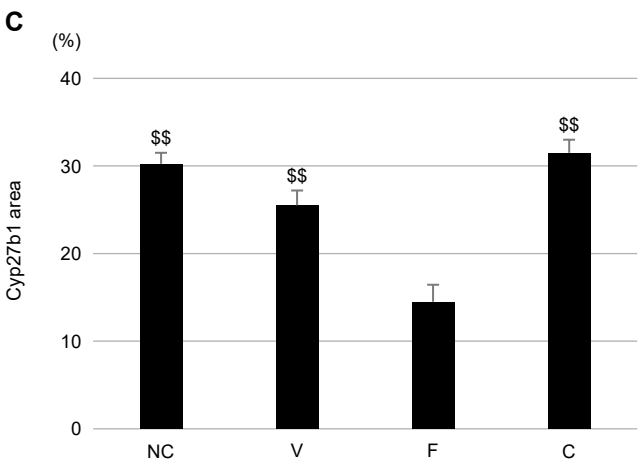
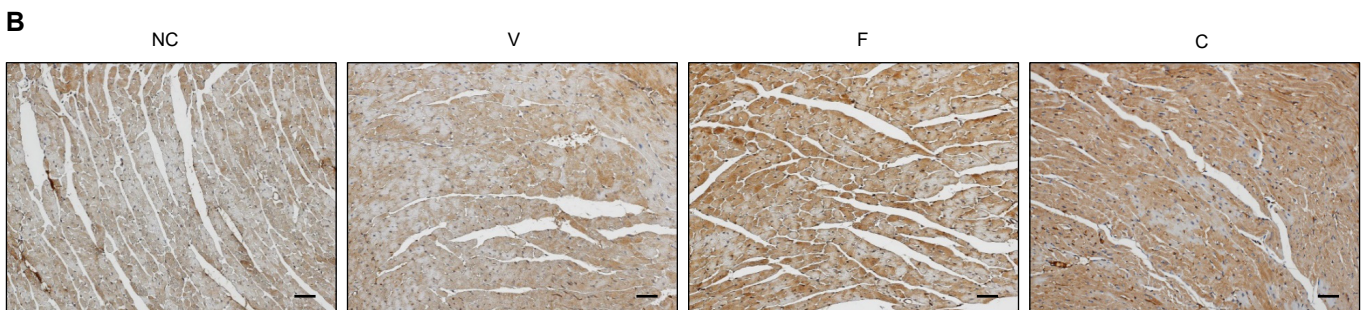
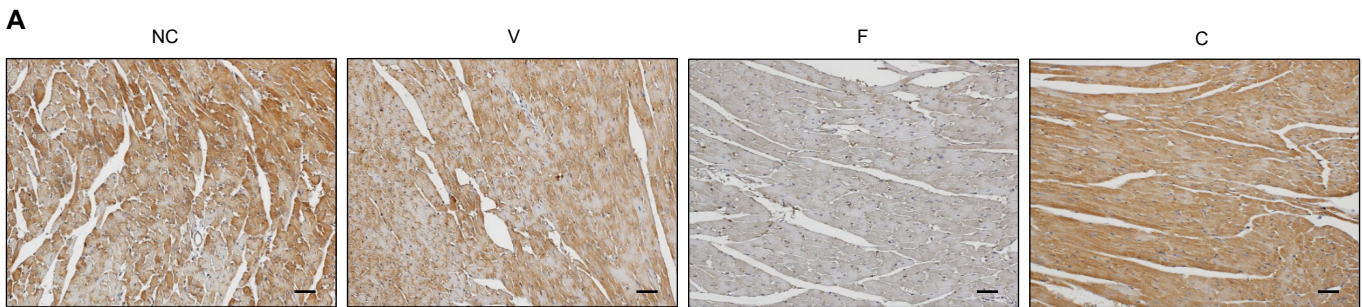
systole; LVPWd, LV posterior wall end diastole; LVPWs, LV posterior wall end systole, LVEF, left

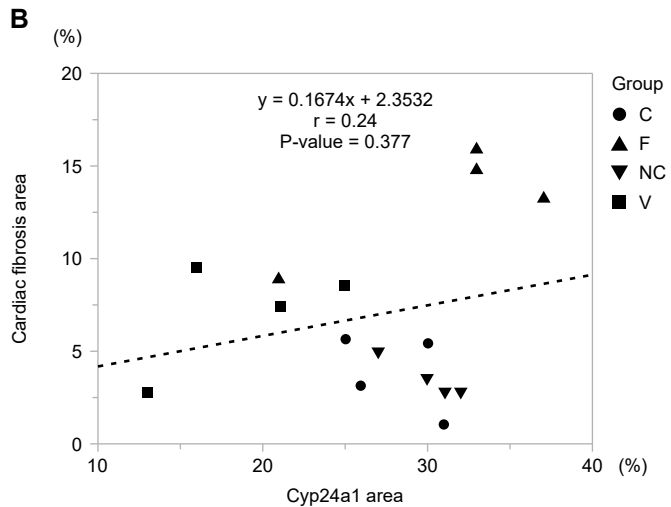
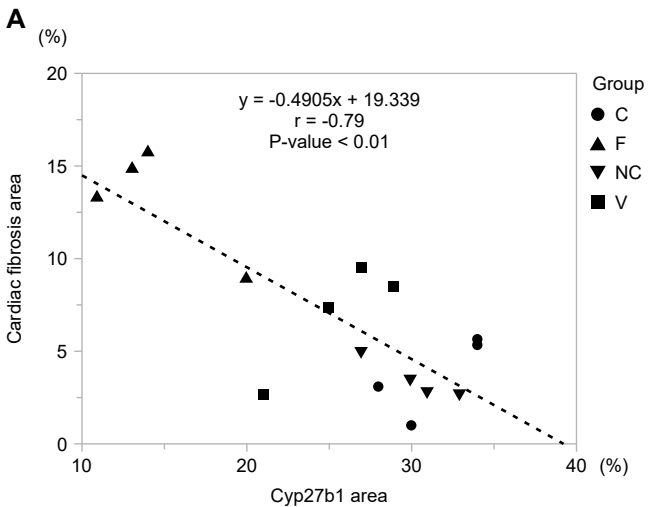
ventricular ejection fraction; and E/A, ratio of peak E velocity to peak A velocity.

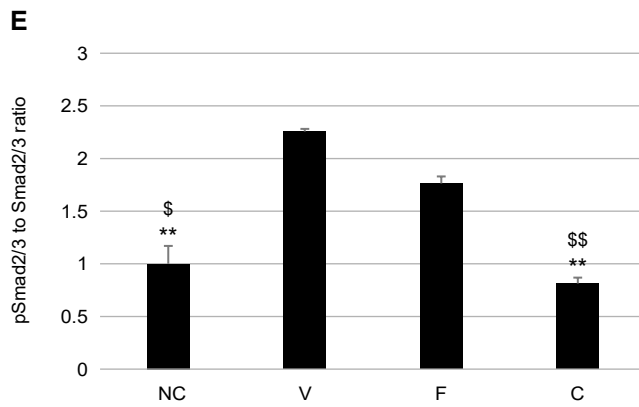
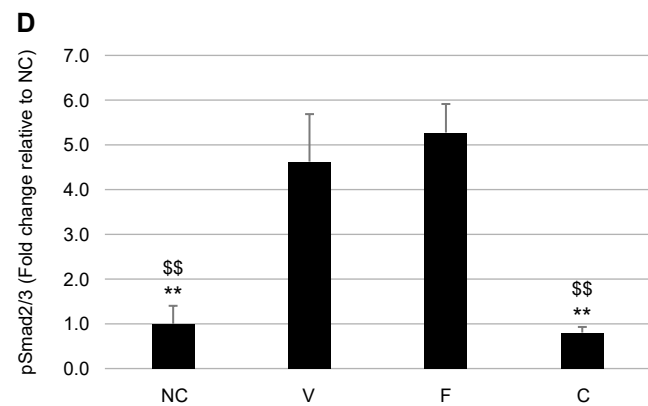
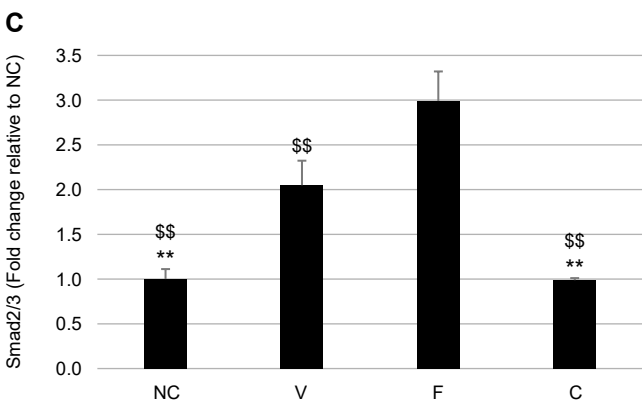
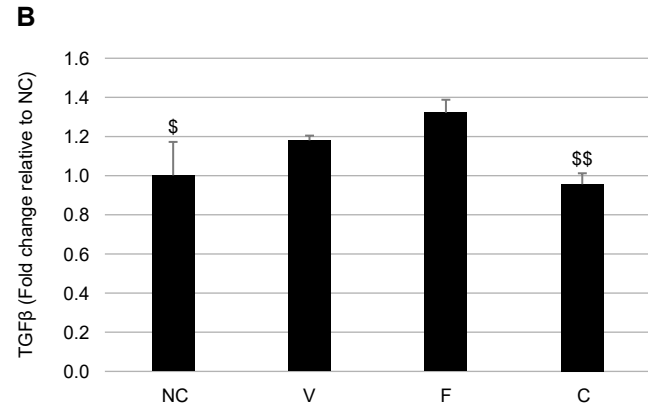
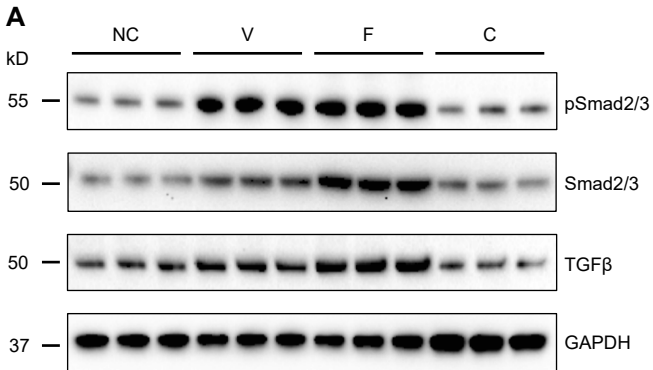


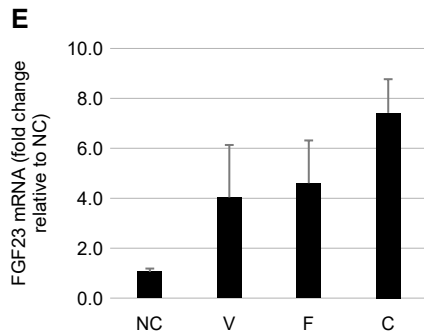
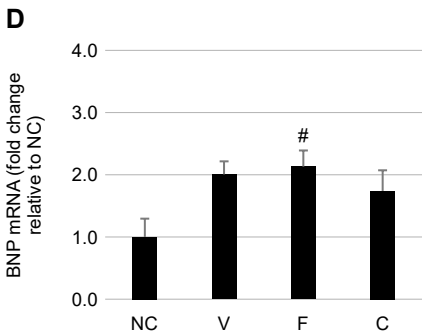
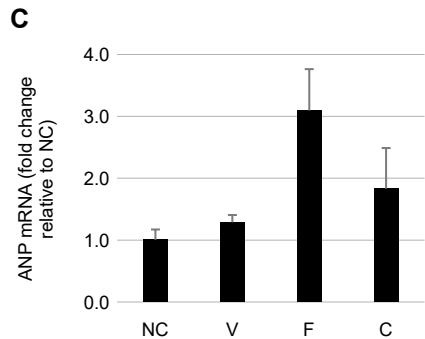
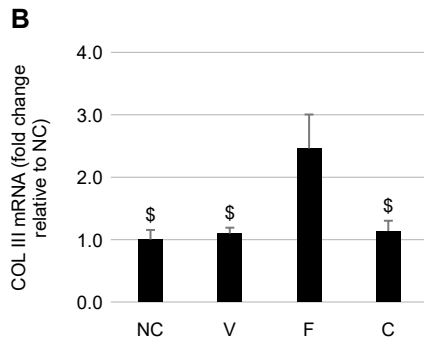
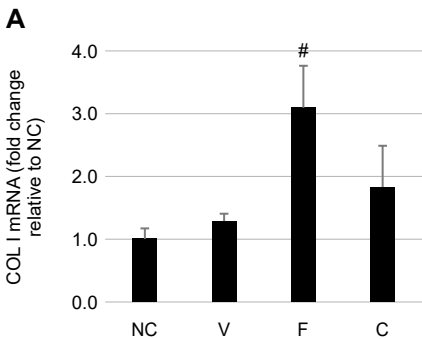


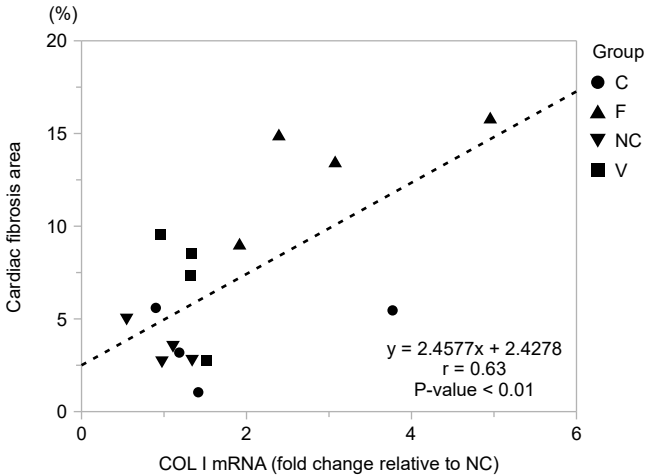










A**B**